In Vivo Active Aldosterone Synthase Inhibitors with Improved Selectivity: Lead Optimization Providing a Series of Pyridine Substituted 3,4-Dihydro-1*H*-quinolin-2-one Derivatives

Simon Lucas,[†] Ralf Heim,[†] Christina Ries,[†] Katarzyna E. Schewe,[†] Barbara Birk,[‡] and Rolf W. Hartmann*[,†]

Pharmaceutical and Medicinal Chemistry, Saarland University, P.O. Box 151150, D-66041 Saarbrücken, Germany, Pharmacelsus CRO, Science Park 2, D-66123 Saarbrücken, Germany

Received July 17, 2008

Pyridine substituted naphthalenes (e.g., **I**−**III**) constitute a class of potent inhibitors of aldosterone synthase (CYP11B2). To overcome the unwanted inhibition of the hepatic enzyme CYP1A2, we aimed at reducing the number of aromatic carbons of these molecules because aromaticity has previously been identified to correlate positively with CYP1A2 inhibition. As hypothesized, inhibitors with a tetrahydronaphthalene type molecular scaffold (**1**−**11**) exhibit a decreased CYP1A2 inhibition. However, tetralone **9** turned out to be cytotoxic to the human cell line U-937 at higher concentrations. Consequent structural optimization culminated in the discovery of heteroaryl substituted 3,4-dihydro-1*H*-quinolin-2-ones (**12**−**26**), with **12**, a bioisostere of **9**, being nontoxic up to 200 μM. The investigated molecules are highly selective toward both CYP1A2 and a wide range of other cytochrome P450 enzymes and show a good pharmacokinetic profile in vivo (e.g., **12** with a peroral bioavailability of 71%). Furthermore, isoquinoline derivative **21** proved to significantly reduce plasma aldosterone levels of ACTH stimulated rats.

Introduction

The progressive nature of congestive heart failure (CHF[a]) is a consequence of a neurohormonal imbalance that involves a chronic activation of the renin−angiotensin−aldosterone system (RAAS) in response to reduced cardiac output and reduced renal perfusion. Aldosterone and angiotensin II (Ang II) are excessively released, leading to increased blood volume and blood pressure as a consequence of epithelial sodium retention as well as Ang II mediated vasoconstriction and finally to a further reduction of cardiac output.[1] The RAAS is pathophysiologically stimulated in a vicious cycle of neurohormonal activation that counteracts the normal negative feedback loop regulation. The most important circulating mineralocorticoid, aldosterone, acts by binding to specific mineralocorticoid receptors (MR) located in the cytosol of target epithelial cells. Thereby, renal sodium reabsorption and potassium secretion are promoted in the distal tubule and the collecting duct of the nephron. Elevated blood volume and thus blood pressure result from water that follows the sodium movement via osmosis. In addition to these indirect effects on the heart function, aldosterone exerts direct effects on the heart by activating nonepithelial MRs in cardiomyocytes, fibroblasts, and endothelial cells. Synthesis and deposition of fibrillar collagen in the fibroblasts result in myocardial fibrosis.[2] Relatively inelastic collagen fibers stiffen the heart muscle, which deteriorates the myocardial function and as a consequence enhances the neurohormonal imbalance by further stimulation of the RAAS. In addition to the effects of circulating aldosterone deriving from adrenal secretion, Satoh et al. reported that aldosterone produced locally in the heart triggers myocardial fibrosis, too.[3] Recent clinical studies with the MR antagonists spironolactone and eplerenone gave evidence for the pivotal role of aldosterone in the progression of cardiovascular diseases. Blocking the aldosterone action by functional antagonism of its receptor reduced the mortality and significantly reduced the symptoms of heart failure.[4] Furthermore, follow-up studies revealed that cardiac fibrosis can not only be prevented but also reversed by use of spironolactone.[5]

However, several issues are unsolved by this therapeutic strategy. Spironolactone binds rather unselectively to the aldosterone receptor and also has some affinity to other steroid receptors, provoking adverse side effects.[4] Although eplerenone is more selective, clinically relevant hyperkalemia remains a principal therapeutic risk.[6] Another crucial point is the high concentration of circulating aldosterone, which is not lowered by MR antagonistic therapy and raises several issues. First, the elevated aldosterone plasma levels do not induce a homologous down-regulation but an up-regulation of the aldosterone receptor, which complicates a long-term therapy because MR antagonists are likely to become ineffective.[7] Furthermore, the nongenomic actions of aldosterone are in general not blocked by receptor antagonists and can occur despite MR antagonistic treatment.[8] A novel therapeutic strategy for the treatment of hyperaldosteronism, congestive heart failure, and myocardial fibrosis with potential to overcome the drawbacks of MR antagonists was recently suggested by us:[9,10] blockade of aldosterone production by inhibiting the key enzyme of its biosynthesis, aldosterone synthase (CYP11B2), a mitochondrial cytochrome P450 enzyme that is localized mainly in the adrenal cortex and catalyzes the terminal three oxidation steps in the biogenesis of aldosterone in humans.[11] Consequent structural optimization of a hit discovered by compound library screening led to a series of nonsteroidal aldosterone synthase inhibitors with high selectivity versus other cytochrome P450 enzymes.[12,13] Pyridine-substituted naphthalenes[14,15] such as **I**−**III** (Chart 1) and dihydronaphthalenes,[16] the most potent and selective compounds that emerged from our drug discovery program, however, revealed two major

* To whom correspondence should be addressed. Phone: +49 681 302 2424. Fax: +49 681 302 4386. E-mail: rwh@mx.uni-saarland.de.

[†] Pharmaceutical and Medicinal Chemistry, Saarland University.

[‡] Pharmacelsus CRO.

[a] Abbreviations: ACTH, adrenocorticotrophic hormone; Ang II, angiotensin II; AUC, area under the curve; CHF, congestive heart failure; CYP, cytochrome P450; CYP11B1, 11β-hydroxylase; CYP11B2, aldosterone synthase; CYP17, 17α-hydroxylase-17,20-lyase; CYP19, aromatase; Het, heteroaryl; KHMDS, potassium hexamethyldisilazane; MR, mineralocorticoid receptor; NBS, *N*-bromosuccinimide; NCS, *N*-chlorosuccinimide; PPB, plasma protein binding; RAAS, renin−angiotensin−aldosterone system; Tf_2NPh, *N*-phenyltrifluoromethanesulphonimide.

10.1021/jm800888q CCC: $40.75
Published on Web 12/02/2008

Chart 1. Pyridylnaphthalene Type CYP11B2 Inhibitors **I**−**III** and Design Strategy for 3,4-Dihydro-1*H*-quinolin-2-one Derivatives (e.g., **12** and **14**)

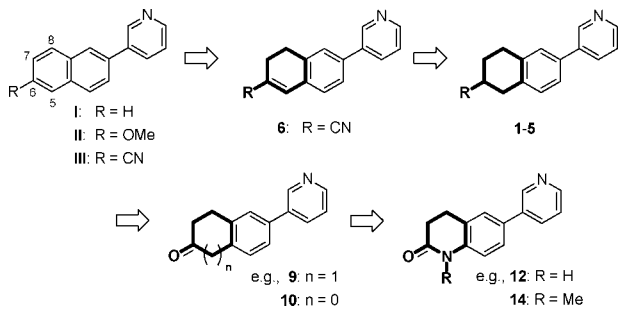

Chart 2. Title Compounds: Pyridine Substituted 3,4-Dihydro-1*H*-quinolin-2-one Derivatives and Structurally Related Compounds

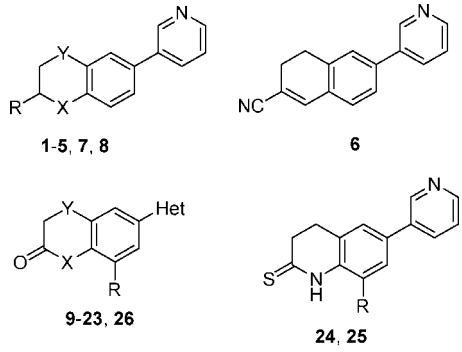

pharmacological drawbacks: a strong inhibition of the hepatic drug metabolizing enzyme CYP1A2 and no inhibitory effect on the aldosterone production in vivo by using a rat model.

In the present study, we describe the design and the synthesis of pyridine-substituted 3,4-dihydro-1*H*-quinolin-2-ones and structurally related compounds as highly potent and selective CYP11B2 inhibitors (Chart 2). The design concept toward these molecules is based on a systematic reduction of aromaticity by saturation of the hydrocarbons C_5 to C_8 of the naphthalene moiety and subsequent chemical modification of the fully saturated ring (Chart 1). The inhibitory activity of the title compounds was determined in V79 MZh cells expressing human CYP11B2. The selectivity was investigated with respect to the highly homologous 11β-hydroxylase (CYP11B1) as well as other crucial steroid- or drug-metabolizing cytochrome P450 enzymes (CYP17, CYP19, CYP1A2, CYP2B6, CYP2C9, CYP2C19, CYP2D6, and CYP3A4). The in vivo pharmacokinetic profile of some promising compounds was determined in male Wistar rats in both cassette and single dosing experiments. Furthermore, plasma protein binding and cytotoxicity studies were performed. The isoquinoline derivative **21** was investigated for aldosterone lowering effects in vivo using ACTH stimulated rats.

Results

Chemistry. The key step for the synthesis of the title compounds was a Suzuki coupling to introduce the heterocycle, mostly 3-pyridine. In case of the unsubstituted tetrahydronaphthalene **1**, the cross-coupling was accomplished by a microwave enhanced method[17] using 3-pyridineboronic acid and triflate **1a**, which was prepared from the corresponding tetrahydronaphthol (Scheme 1).[18] Compounds **7**, **8**, and **26** were synthesized via Suzuki coupling from commercially available arylbromides and 3-pyridineboronic acid under microwave heating.

Scheme 1[a]

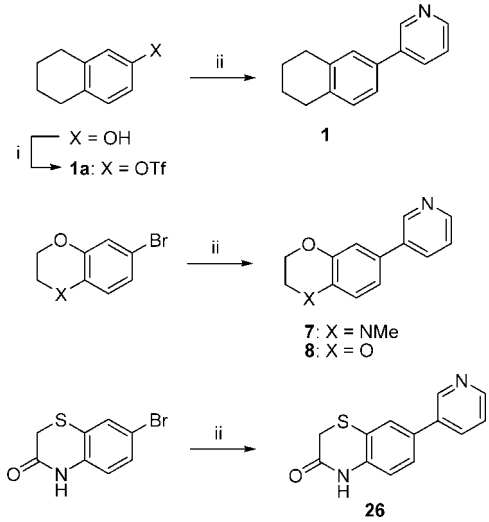

[a] Reagents and conditions: (i) Tf_2NPh, K_2CO_3, THF, μw, 120 °C; (ii) 3-pyridineboronic acid, $Pd(PPh_3)_4$, aq $NaHCO_3$, DMF, μw, 150 °C.

The synthesis of compounds **2**−**6** and **9**−**11** (Scheme 2) started from either 6-bromo-2-tetralone ($n = 1$) or 5-bromo-1-indanone ($n = 0$) as key building blocks. Suzuki coupling afforded the heterocycle-substituted analogues **9**−**11**. Dihydronaphthalene derivative **6** was prepared by treatment of tetralone **9** with KHMDS, in situ quenching the enolate with Tf_2NPh,[19] and Pd-catalyzed cyanation[20] of the intermediate enoltriflate. The hydroxy-substituted tetrahydronaphthalene **2** was obtained by sodium borohydride reduction of the carbonyl group[21] to afford **2a** and subsequent Suzuki coupling. *O*-Alkylation of **2** afforded the corresponding methoxy- (**3**) and ethoxy-substituted (**4**) derivatives. The 6-cyano-derivatized analogue **5** was prepared in three consecutive steps starting with a one-pot cyanohydrin/elimination step.[22] The intermediate α,β-unsaturated nitrile **5b** was treated with $NaBH_4$ in refluxing ethanol to reduce the double bond.[23] Suzuki coupling of **5a** with 3-pyridineboronic acid afforded the tetrahydronaphthalene **5**.

The synthesis of the compounds with a dihydro-1*H*-quinolin-2-one and structurally related scaffold was accomplished as outlined in Scheme 3. The initial bromination procedures yielding either **12a** or **13a** have been described previously.[24,25] Subsequent *N*-alkylation was accomplished by treating the quinolinones with alkyl halide and potassium *tert*-butylate in dimethylformamide to afford the intermediates **14a**−**16a**.[26] A nitro substituent was selectively introduced in the 8-position of **10a** by treating with a mixture of concentrated sulfuric acid and concentrated nitric acid to yield **18a**.[27] The obtained bromoarenes were transformed into the heterocycle-substituted analogues **12**−**16** and **18**−**23** by Suzuki coupling. Treating **12** with *N*-chlorosuccinimide in dimethylformamide afforded the 8-chloro derivative **17** as the only regioisomer. Conversion of the dihydroquinolinones **12** and **17** into the thio analogues **24** and **25** was carried out using Lawessons reagent in refluxing toluene.

Biology. Inhibition of Human Adrenal Corticoid Producing CYP11B2 and CYP11B1 In Vitro (Table 1). The inhibitory activities of the compounds were determined in V79 MZh cells expressing either human CYP11B2 or CYP11B1.[10,28] The V79 MZh cells were incubated with [^{14}C]-deoxycorticosterone as substrate and the inhibitor in different concentrations. The product formation was monitored by HPTLC using a phosphoimager. Fadrozole, an aromatase (CYP19) inhibitor with

Scheme 2[a]

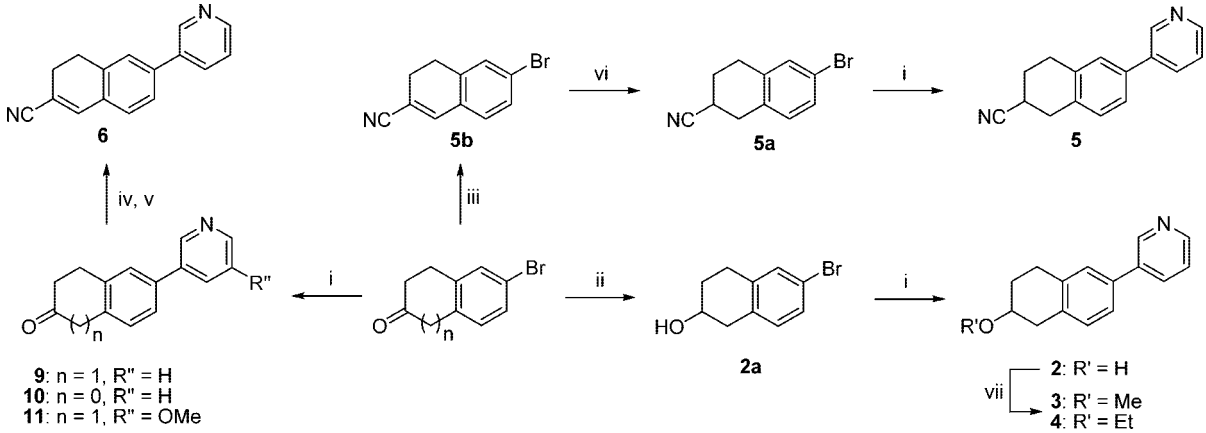

[a] Reagents and conditions: (i) heteroarylboronic acid, $Pd(PPh_3)_4$, aq $NaHCO_3$, DMF, μw, 150 °C; (ii) $NaBH_4$, methanol, 0 °C; (iii) Me_3SiCN, ZnI_2, toluene, rt, then $POCl_3$, pyridine, reflux; (iv) Tf_2NPh, KHMDS, THF/toluene, −78 °C; (v) $Zn(CN)_2$, $Pd(PPh_3)_4$, DMF, 100 °C; (vi) $NaBH_4$, ethanol, reflux; (vii) alkyl halide, NaH, THF, 50 °C.

Scheme 3[a]

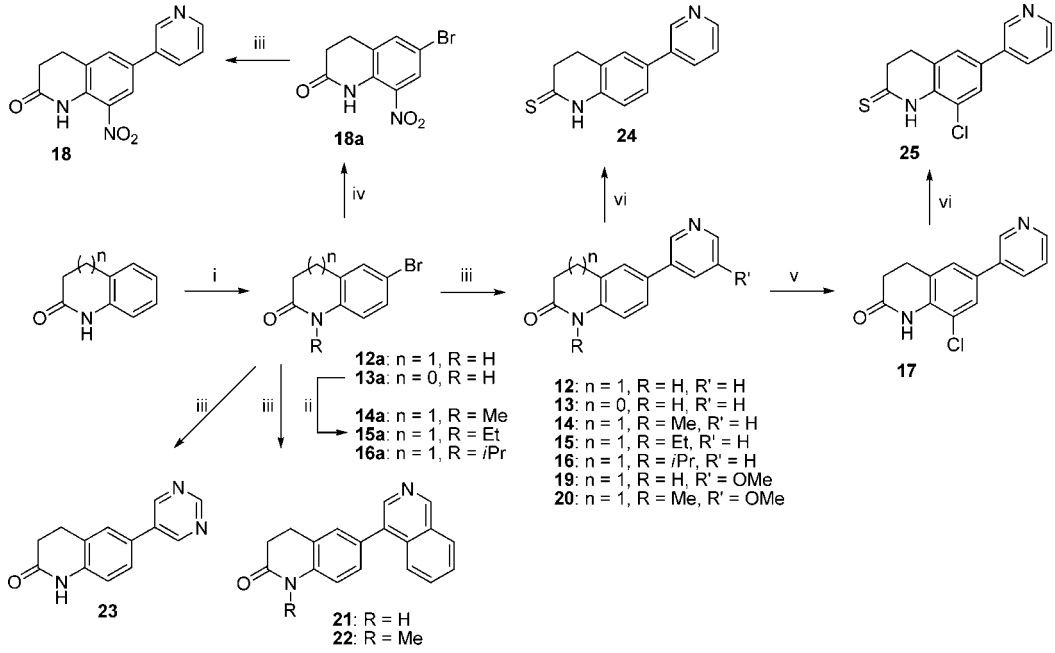

[a] Reagents and conditions: (i) NBS, DMF, 0 °C ($n = 1$) or Br_2, KBr, water, reflux ($n = 0$); (ii) alkyl halide, KO*t*Bu, DMF, rt; (iii) heteroarylboronic acid, $Pd(PPh_3)_4$, aq $NaHCO_3$, DMF, μw, 150 °C or $Pd(PPh_3)_4$, aq Na_2CO_3, toluene/ethanol, reflux; (iv) HNO_3/H_2SO_4, rt; (v) NCS, DMF, 65 °C; vi) Lawesson's reagent, toluene, reflux.

ability to reduce corticoid formation in vitro[29] and in vivo,[30] was used as a reference (CYP11B2, $IC_{50} = 1$ nM; CYP11B1, $IC_{50} = 10$ nM).

Most of the compounds presented in Table 1 show a strong inhibition of the target enzyme. Within the tetrahydro- and dihydronaphthalene series (compounds **1**−**6**), a substituent in 6-position of the carbocyclic skeleton induces an increased inhibitory potency in case of methoxy- (compound **3**) and cyano-substituents (compounds **5**, **6**) as well as a dramatic increase in selectivity toward CYP11B1, most notably in methoxy derivative **3** (selectivity factor = 347). Contrariwise, introduction of heteroatoms into the saturated ring leads to a decrease of CYP11B2 inhibition (e.g., **7** and **8**). The carbonyl derivatives **9**−**11** are also highly potent ($IC_{50} = 1.8$−7.8 nM) and selective aldosterone synthase inhibitors. Tetralone **9** is the most selective compound of the present series displaying a CYP11B1 IC_{50} value 496-fold higher than the CYP11B2 IC_{50} value. The derivatives with dihydro-1*H*-quinolin-2-one molecular scaffold (**12**−**26**) exhibit a range of both inhibitory potency at the target enzyme ($IC_{50} = 0.1$−64 nM) and selectivity with respect to CYP11B1 inhibition (selectivity factor = 44−440). A significant decrease in inhibitory potency can be observed for derivatization of the lactam nitrogen by an isopropyl residue (compound **16**), whereas methyl (compound **14**) and ethyl (compound **15**) are tolerated in this position. The activity also decreases when the 3-pyridine is replaced by the 5-pyrimidine (compound **23**) as the heterocyclic moiety. Introduction of a nitro substituent in the 8-position results in the rather moderate CYP11B2 inhibitor **18** ($IC_{50} = 64$ nM) with lower CYP11B1 selectivity. Contrariwise, a chloro substituent in the same position (compound **17**) increases the inhibitory potency by a factor of 7 compared to the hydrogen analogue **12**. The most potent inhibitors are obtained when the 3-pyridine moiety is modified by 5-methoxylation or replaced by 4-isoquinoline, resulting in subnanomolar IC_{50} values for compounds **20**−**22** ($IC_{50} = 0.1$−0.2 nM). Isoquinoline derivative **22** displays an IC_{50} value as low as 0.1

Table 1. Inhibition of Human Adrenal CYP11B2 and CYP11B1 In Vitro

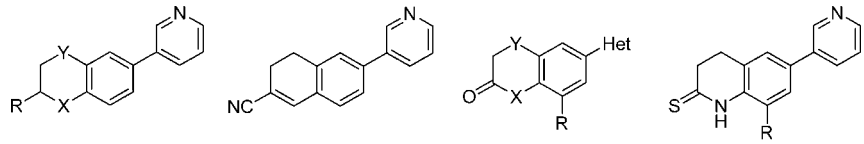

1-5, **7**, **8** **6** **9-23**, **26** **24**, **25**

					% inhibition[a]	IC$_{50}$ value[b] (nM)		
compd	R	X	Y	Het	V79 11B2[c] hCYP11B2	V79 11B2[c] hCYP11B2	V79 11B1[d] hCYP11B1	selectivity factor[e]
1	H	CH_2	CH_2		82	29	1977	68
2	OH	CH_2	CH_2		86	44	4921	112
3	OMe	CH_2	CH_2		97	3.3	1145	347
4	OEt	CH_2	CH_2		92	30	4371	146
5	CN	CH_2	CH_2		94	5.1	745	146
6					97	1.6	290	181
7	H	NMe	O		71	101	5970	59
8	H	O	O		70	154	13378	87
9	H	CH_2	CH_2	3-pyridine	97	7.8	3964	496
10	H		CH_2	3-pyridine	90	4.4	819	186
11	H	CH_2	CH_2	5-methoxy-3-pyridine	94	1.8	191	106
12	H	NH	CH_2	3-pyridine	88	28	6746	241
13	H	NH		3-pyridine	85	14	5952	425
14	H	NMe	CH_2	3-pyridine	92	2.6	742	289
15	H	NEt	CH_2	3-pyridine	93	22	5177	235
16	H	N*i*Pr	CH_2	3-pyridine	39	nd	nd	nd
17	Cl	NH	CH_2	3-pyridine	97	3.8	1671	440
18	NO_2	NH	CH_2	3-pyridine	78	64	5402	84
19	H	NH	CH_2	5-methoxy-3-pyridine	91	2.7	339	126
20	H	NMe	CH_2	5-methoxy-3-pyridine	94	0.2	87	435
21	H	NH	CH_2	4-isoquinoline	94	0.2	33	187
22	H	NMe	CH_2	4-isoquinoline	99	0.1	6.9	69
23	H	NH	CH_2	5-pyrimidine	57	nd	nd	nd
24	H				97	3.1	580	187
25	Cl				97	4.2	769	183
26	H	NH	S	3-pyridine	92	12	525	44
fadrozole						1.0	10	10

[a] Mean value of at least four experiments, standard deviation less than 10%; inhibitor concentration, 500 nM. [b] Mean value of at least four experiments, standard deviation usually less than 25%, nd = not determined. [c] Hamster fibroblasts expressing human CYP11B2; substrate deoxycorticosterone, 100 nM. [d] Hamster fibroblasts expressing human CYP11B1; substrate deoxycorticosterone, 100 nM. [e] IC$_{50}$ CYP11B1/IC$_{50}$ CYP11B2, nd = not determined.

nM and is the most potent aldosterone synthase inhibitor known so far and also shows a pronounced inhibitory potency at CYP11B1 (IC$_{50}$ = 6.9 nM). The same trend was observed previously for the binding properties of a series of heteroaryl-substituted naphthalenes.[31] Changing the lactam moiety into the corresponding thiolactam results in a slightly reduced CYP11B1 selectivity as seen in compounds **24** and **25** compared to the oxygen analogues **12** and **17**. Moreover, incorporation of a sulfur atom into the lactam moiety in compound **26** induces a dramatic loss of CYP11B1 selectivity (selectivity factor = 44).

Inhibition of Steroidogenic and Hepatic CYP Enzymes (Tables 2 and 3). The inhibition of CYP17 was investigated using the 50000*g* sediment of the *E. coli* homogenate recombinantly expressing human CYP17 and progesterone (25 μM) as substrate.[32] The percent inhibition values were measured at an inhibitor concentration of 2.5 μM. Most of the investigated compounds display rather low inhibitory action on CYP17 (Table 2). However, a distinct inhibition in the range of 31−74% at a concentration of 2.5 μM is observed in case of the tetrahydro- and dihydronaphthalenes **2**−**6**, which is comparable to the naphthalene parent compounds **I**−**III** (40−73%). All other derivatives, including the keto analogues **9**−**11** and the investigated dihydro-1*H*-quinolin-2-ones, are considerably less active at CYP17 (<22%). Exceptions from this are lactam **12** (41% inhibition) and the thiolactam analogue **24** (72%). The inhibition of CYP19 at a concentration of 500 nM was determined in vitro with human placental microsomes and [1β-^{3}H]androstenedione as substrate as described by Thompson and Siiteri[33] using our

Table 2. Inhibition of Human CYP17, CYP19, and CYP1A2 In Vitro

	% inhibition[a] [IC$_{50}$ value[b] (μM)]		
compd	CYP17[c]	CYP19[d]	CYP1A2[e]
I	40	[5.7]	99 [nd]
II	72	[0.6]	98 [nd]
III	73	[>36]	97 [nd]
2	49	23	74 [0.60]
3	44	22	80 [0.44]
4	31	10	73[0.62]
5	38	<5	72 [0.66]
6	74	<5	90 [0.18]
9	20	31	60 [1.55]
10	<5	53	57 [1.55]
11	21	58	57 [1.56]
12	41	21	50 [1.95]
13	<5	62	25 [6.58]
14	8	54	53 [1.79]
15	<5	63	36 [3.48]
17	7	17	14 [30.6]
19	12	<5	25 [5.24]
20	<5	5	20 [16.5]
21	22	<5	<5 [>150]
24	72	<5	77 [0.64]

[a] Mean value of three experiments, standard deviation less than 10%. [b] Mean value of two experiments, standard deviation less than 5%. [c] *E. coli* expressing human CYP17; substrate progesterone, 25 μM; inhibitor concentration, 2.5 μM; ketoconazole, IC$_{50}$ = 2.78 μM. [d] Human placental CYP19; substrate androstenedione, 500 nM; inhibitor concentration, 500 nM; fadrozole, IC$_{50}$ = 30 nM. [e] Recombinantly expressed enzymes from baculovirus-infected insect microsomes (Supersomes); inhibitor concentration, 2.0 μM; furafylline, IC$_{50}$ = 2.42 μM.

Table 3. Inhibition of Selected Hepatic CYP Enzymes In Vitro

compd	IC_{50} value[a] (μM)				
	CYP 2B6[b,c]	CYP 2C9[b,d]	CYP 2C19[b,e]	CYP 2D6[b,f]	CYP 3A4[b,g]
3	47.4	16.3	<200	<200	12.2
9	<50	28.3	41.5	171	6.21
10	<50	123	147	<200	<200
11	<50	12.9	45.4	<200	3.8
12	<50	58.9	<200	171	127
14	<50	125	122	<200	<200
21	<100	2.9	9.2	<50	<50

[a] Mean value of two experiments, standard deviation less than 5%. [b] Recombinantly expressed enzymes from baculovirus-infected insect microsomes (Supersomes). [c] Tranylcypromine, $IC_{50} = 6.24$ μM. [d] Sulfaphenazole, $IC_{50} = 318$ nM. [e] Tranylcypromine, $IC_{50} = 5.95$ μM. [f] Quinidine, $IC_{50} = 14$ nM. [g] Ketoconazole, $IC_{50} = 57$ nM.

modification.[34] In most cases, the inhibitory action on CYP19 is low (<30%) at the chosen concentration (Table 2). Exceptions are observed in case of the keto derivatives **10** and **11** as well as the lactam derivatives **13**−**15**, displaying aromatase inhibition in the range of 53−63%.

A selectivity profile relating to inhibition of crucial hepatic CYP enzymes (CYP1A2, CYP2B6, CYP2C9, CYP2C19, CYP2D6, and CYP3A4) was determined by use of recombinantly expressed enzymes from baculovirus-infected insect microsomes. As previous studies have shown that aldosterone synthase inhibitors of the naphthalene type are potent inhibitors of CYP1A2 but otherwise rather selective versus important hepatic CYP enzymes,[14,15] most of the newly prepared compounds were initially tested for their inhibitory action on CYP1A2 (Table 2). The parent compounds **I**−**III** are highly potent inhibitors of CYP1A2 (>95% inhibition at concentration of 2 μM). With regard to this high CYP1A2 activity of these naphthalene type compounds, the inhibitory potency slightly decreases in case of the dihydronaphthalene derivative **6** (90%) and the tetrahydronaphthalene derivatives **2**−**5** (72−80%). The keto analogues **9**−**11** exhibit 57−60% inhibition corresponding with IC_{50} values of approximately 1.6 μM. A further decrease of CYP1A2 inhibition to less than 55% is observed for the investigated lactam bioisosteres **12**−**15**, **17**, and **19**−**21**. This is especially true for chloro-substituted **17** as well as compounds **20** and **21** with modified heterocycles displaying IC_{50} values greater than 15 μM but also for indanone **13** and methoxypyridine derivative **19** with IC_{50} values greater than 5 μM. However, compound **24**, the thio analogue of **12**, displays a pronounced inhibitory potency ($IC_{50} = 0.64$ μM). Some compounds were also scrutinized for inhibition of other crucial hepatic CYP enzymes (Table 3). The data presented in Table 3 reveal that the investigated CYP enzymes are rather unaffected by the compounds with tetrahydronaphthalene (**3**), tetralone (**9**−**11**), as well as dihydro-1*H*-quinolin-2-one (**12**, **14**, and **21**) type molecular scaffold, and with few exceptions (i.e., **9**, **11** at CYP3A4 and **21** at CYP2C9) the IC_{50} values measured are significantly greater than 10 μM.

Plasma Protein Binding (Table 4). The plasma protein binding of compounds **9**, **10**, and **12** was determined by ultrafiltration. Test solutions of an aliquot of concentrated test compound and rat or human plasma were incubated at 37 °C for 1 h and then centrifuged at 8000*g* for 20 min. Ultrafiltrates were analyzed for drug concentrations by LC-MS/MS. The plasma protein binding of the investigated CYP11B2 inhibitors was found to be low. The bound form of keto compounds **9** and **10** range between 22−25% in both human and rat plasma. In the case of the bioisosteric dihydro-1*H*-quinolin-2-one **12**, the amount of freely available compound is lower (approximately 60% bound).

Table 4. Plasma Protein Binding of Compounds **9**, **10**, and **12**

compd	PPB[a] (% bound)	
	rat	human
9	25	24
10	24	22
12	60	61

[a] Determined by analysis of the ultrafiltrates via LC-MS/MS; the degree of binding to the plasma proteins (PPB) is calculated by the following equation: % PPB = $(1 - [\text{ligand}_{\text{ultrafiltrate}}]/[\text{ligand}_{\text{total}}]) \cdot 100$.

Table 5. Pharmacokinetic Profile of Compounds **9**−**12**, **14**, and **21**

compd	dose (mg/kg)[a]	$t_{1/2\,z}$ (h)[b]	t_{max} (h)[c]	C_{max} (ng/mL)[d]	$AUC_{0-\infty}$ (ng·h/mL)[e]
9[f]	5	3.5	4	104	727
10[f]	5	2.4	4	300	3178
11[f]	5	3.9	4	35	212
12[f,g]	5	3.8	4	261	1753
12	25	1.2	1	1537	4762
12	1[h]	1.7			270
14[f]	5	2.3	6	86	659
21	25	2.9	2	134	1658
fadrozole[f,g]	5	3.2	1	471	3207

[a] Compounds were applied perorally to male Wistar rats. [b] Terminal half-life. [c] Time of maximal concentration. [d] Maximal concentration. [e] Area under the curve. [f] These compounds were investigated in a cassette dosing approach. [g] Mean value of two experiments. [h] Intravenous application.

In Vivo Pharmacokinetics (Table 5). The pharmacokinetic profile of selected compounds was determined after peroral application to male Wistar rats. Plasma samples were collected over 24 h and plasma concentrations were determined by HPLC-MS/MS. Compounds **9**−**12** and **14** were investigated in cassette dosing experiments (peroral dose = 5 mg/kg) and compared to fadrozole. All five compounds show comparable absorption rates ($t_{max} = 4-6$ h) and terminal half-lifes ($t_{1/2z} = 2.3-3.9$ h). The slowest elimination is observed in case of tetralone **11** ($t_{1/2z} = 3.9$ h) and dihydro-1*H*-quinolin-2-one **12** ($t_{1/2z} = 3.8$ h). Within this series, compound **10** shows the highest maximal concentration (C_{max}) in plasma (300 ng/mL), followed in the same range by compound **12** (261 ng/mL). Using the area under the curve ($AUC_{0-\infty}$) as a ranking criterion, the bioavailability after peroral cassette dosing increases in the order **11** (212 ng·h/mL) < **14** (659 ng·h/mL) < **9** (727 ng·h/mL) < **12** (1753 ng·h/mL) < **10** (3178 ng·h/mL). Compounds **12** and **21** were investigated in single dosing experiments (peroral dose = 25 mg/kg). The amounts of the test compounds found in the plasma after peroral application are rather high in case of **21** ($AUC_{0-\infty} = 1658$ ng·h/mL) and high in case of **12** ($AUC_{0-\infty} = 4762$ ng·h/mL). Comparing the AUC of peroral with intravenous (dose = 1 mg/kg) application of dihydro-1*H*-quinolin-2-one **12** reveals an absolute bioavailability of 71%. Although the maximal concentration of **21** found in the plasma is significantly lower than in the case of compound **12** (factor 11), the $AUC_{0-\infty}$ values differ only by a factor of 3, which is due to the greater terminal half-life of isoquinoline derivative **21**. This becomes particularly apparent from Figure 1, where the mean profile of plasma levels (ng/mL) in rat versus time after oral application (25 mg/kg) of compounds **12** (Figure 1a) and **21** (Figure 1b) are shown. The concentrations of **21** are rather constant and measure between 90−130 ng/mL in a time frame of 0.5−8 h after application,

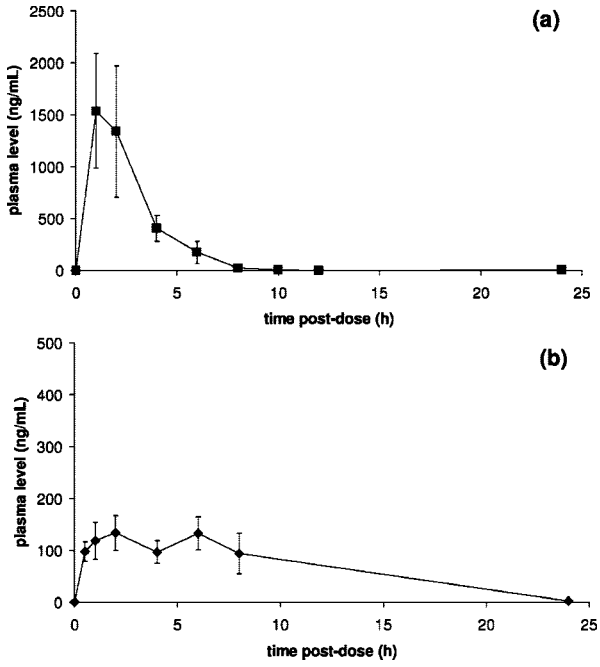

Figure 1. Mean profile (±) SEM of plasma levels (ng/mL) in rat versus time after oral application (25 mg/kg) of compounds **12** (a) and **21** (b) determined in single dosing experiments.

albeit the plasma levels are considerably lower than the plasma levels of **12**.

Discussion and Conclusion

Selectivity is a prerequisite of any drug candidate to avoid adverse side effects. In the development process of aldosterone synthase inhibitors, it is a crucial point to investigate the selectivity profile toward other cytochrome P450 enzymes at an early stage. It is known that the concept of heme-iron complexation (e.g., by nitrogen-containing heterocycles) is an appropriate strategy to discover highly potent and selective inhibitors. Because of this binding mechanism, however, a putative CYP11B2 inhibitor is potentially capable of interacting with other CYP enzymes by similarly binding to the heme cofactor with its metal binding moiety. Taking into consideration that the key enzyme of glucocorticoid biosynthesis, 11β-hydroxylase (CYP11B1), and CYP11B2 have a sequence homology of approximately 93%,[35] the selectivity issue is especially critical for the design of CYP11B2 inhibitors. Recently, we have demonstrated that 3-pyridine substituted naphthalenes such as **I**−**III** provide an ideal molecular scaffold for high inhibitory potency at the target enzyme CYP11B2 as well as high selectivity toward several other CYP enzymes (e.g., CYP11B1, CYP17, CYP19).[14] However, these compounds strongly inhibit the hepatic enzyme CYP1A2 (e.g., compounds **I**−**III** in Table 2) that makes up about 10% of the overall cytochrome P450 content in the liver and metabolizes aromatic and heterocyclic amines as well as polycyclic aromatic hydrocarbons. In recent QSAR studies, CYP1A2 inhibition has been identified to correlate positively with aromaticity and lipophilicity.[36] Furthermore, both CYP1A2 substrates and inhibitors are usually small-volume molecules with a planar shape (e.g., caffeine[37] and furafylline[38]). Rationalizing these findings, our design strategy aimed at reducing the aromaticity and disturbing the planarity of the molecules while keeping the pharmacophoric points[39] of the naphthalene molecular scaffold (see Chart 1).

These considerations led to the development of pyridine substituted dihydro- and tetrahydronaphthalenes **1**−**6**. The

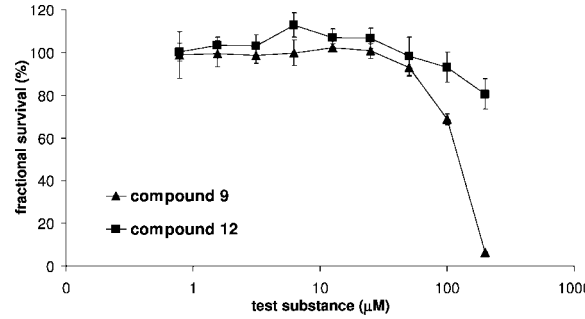

Figure 2. Mean profile (±) SEM of fractional survival (%) of human U-937 cells in presence of compounds **9** or **12**.

compounds are potent aldosterone synthase inhibitors with pronounced selectivity toward CYP11B1. As hypothesized, a decrease of CYP1A2 inhibition can be observed with decreased aromaticity (i.e., number of aromatic carbons) and planarity within this series. While the fully aromatized naphthalenes **I**−**III** exhibit 97−99% inhibition at a concentration of 2 μM, dihydronaphthalene **6** is slightly less potent (90%) and the tetrahydro derivatives **1**−**5** are significantly less potent (72−80%) inhibitors of CYP1A2. However, IC_{50} values are still below 1 μM and thus the molecules are rather strongly inhibiting CYP1A2. Further increase in CYP1A2 selectivity is achieved by introduction of a keto group into the saturated ring as accomplished in compounds **9**−**11**. The inhibitory potencies toward CYP1A2 clearly decrease to IC_{50} values of approximately 1.5 μM. Presumably, the decrease in CYP1A2 inhibition is due to a reduced lipophilicity of the cyclic ketone scaffold compared to the tetrahydronaphthalene scaffold. Lipophilicity has been hypothesized to be one of the most important variables determining CYP1A2 inhibition.[36] Furthermore, the highly potent aldosterone synthase inhibitors **9** (IC_{50} = 7.8 nM) and **10** (IC_{50} = 4.4 nM) show reasonable plasma levels after peroral application to male Wistar rats (Table 5). However, due to the risk of the dialkyl ketone moiety to trigger unwanted cytotoxic effects, tetralone **9** was tested against the human cell line U-937 prior to further optimization. The experiment revealed that this compound significantly reduces the fractional survival of U-937 cells at concentrations greater than 100 μM (Figure 2). Although the cytotoxic effect is seen only at rather high concentrations, which might not play a critical role under physiological conditions, a structural modification of the cyclic ketone moiety was performed with the aim to prevent this potential pharmacological drawback at an early stage by choosing a nontoxic scaffold for further structural modifications. Subsequent bioisosteric exchange by a lactam moiety gave rise to the dihydro-1*H*-quinolin-2-one derivatives **12**−**26**. Contrary to tetralone **9**, dihydro-1*H*-quinolin-2-one **12** exhibits no distinct cytotoxic effect on U-937 cells up to the highest concentration tested (Figure 2). In addition, compound **12** is an even slightly less potent inhibitor of CYP1A2 (IC_{50} = 1.95 μM) than the analogous tetralone (IC_{50} = 1.55 μM), which is again in correspondence with the reduced lipophilicity compared to the bioisosteric **9**. Contrariwise, lipophilicity does not influence the CYP1A2 potency within the series of dihydro-1*H*-quinolin-2-ones (**12**−**21**) as does the substitution pattern of the molecules, especially in the heterocyclic moiety (e.g., **20** and **21**). It is also striking that even minor structural variations such as introduction of a chloro substituent into the dihydro-1*H*-quinolin-2-one core as accomplished in **17** can induce an almost complete loss of CYP1A2 activity.

Pharmacokinetic investigations performed with compound **12** reveal a peroral absolute bioavailability of 71%. Compounds

14 and **21** are also capable of crossing the gastrointestinal tract and reach the general circulation after peroral application. However, their total range of absorption is below that of **12**. The plasma protein binding of inhibitor **12** was found to be low in both rat and human plasma (approximately 60%), indicating that a sizable free fraction of circulating compound is present in the plasma. Within the series of dihydro-1*H*-quinolin-2-one type inhibitors **12**−**26**, most compounds are highly active at the target enzyme. This particularly applies to the derivatives with a functionalized pyridine heterocycle, for example, methoxy derivative **20** (IC_{50} = 0.2 nM) and isoquinoline derivatives **21** (IC_{50} = 0.2 nM) and **22** (IC_{50} = 0.1 nM). By introduction of a chloro substituent in the 8-position or methoxy in the 5-position of the pyridine heterocycle, the selectivity increases to a factor of greater than 400 (**17**, **20**). Hence, these compounds are approximately 40-fold more selective than fadrozole (selectivity factor = 10). With respect to the high homology of the two CYP11B isoforms, this experimental result is particularly noteworthy.

To measure aldosterone-lowering effects in rats, we investigated the most potent and selective inhibitors of the present series for their ability to block aldosterone biosynthesis in V79 MZh cells expressing *rat* CYP11B2 prior to in vivo experiments. The results revealed that only compound **21** (and to a minor degree also the *N*-methyl analogue **22**) shows a moderate inhibitory action toward rat CYP11B2 in vitro, which corroborates our expectations concerning potential problems due to species cross-over, presumably as a consequence of a rather low sequence identity of the human and the rat CYP11B2 enzyme (approximately 69%).[40] The most potent compound in the rat assay, isoquinoline derivative **21**, is also a highly potent inhibitor of human CYP11B2 in vitro (IC_{50} = 0.2 nM) and exhibits a pronounced selectivity toward other CYP enzymes. Examination of availability in plasma following peroral administration of this compound to rats revealed a good half-life (2.9 h) and reasonable plasma levels ($AUC_{0-\infty}$ = 1658 ng·h/mL following a 25 mg/kg dose). For the in vivo study, we used the animal model of Häusler et al., where the animals receive a subcutaneous injection of ACTH (1 mg/kg) 16 h before test item application to stimulate the gluco- and mineralocorticoid biosynthesis and the aldosterone levels are determined using RIA.[40,41] The plasma aldosterone levels of the individual animals of this study are shown in Figure 3. It becomes apparent that ACTH treatment induces a significant increase of the aldosterone levels. Within the vehicle-treated group (animals 7−10, Figure 3b), the concentrations found in the plasma are rather constant over the duration of the experiment (6 h). To six animals (compound **21** group) isoquinoline derivative **21** was intravenously applied in a 20 mg/kg dose after 16 h upon ACTH treatment (animals 1−6, Figure 3a). A significant aldosterone-lowering effect can already be observed after 15 min. Within a time frame of 0.5−3 h, the aldosterone concentrations are maximally reduced to 36−63% of the prior ACTH level for the individual animals of the compound **21** group.

In summary, nonsteroidal aldosterone synthase inhibitors with a dihydro-1*H*-quinolin-2-one molecular scaffold are superior to the previously investigated pyridylnaphthalenes such as **I**−**III**. Most compounds exhibit a potent inhibitory activity at the target enzyme and isoquinoline derivative **22** is the most potent CYP11B2 inhibitor described so far (IC_{50} = 0.1 nM). The selectivity versus other steroidogenic as well as hepatic cytochrome P450 enzymes is generally high. Most notably, the strong inhibition of the hepatic CYP1A2 enzyme (>95% at a concentration of 2 μM) present in the naphthalene type inhibitors

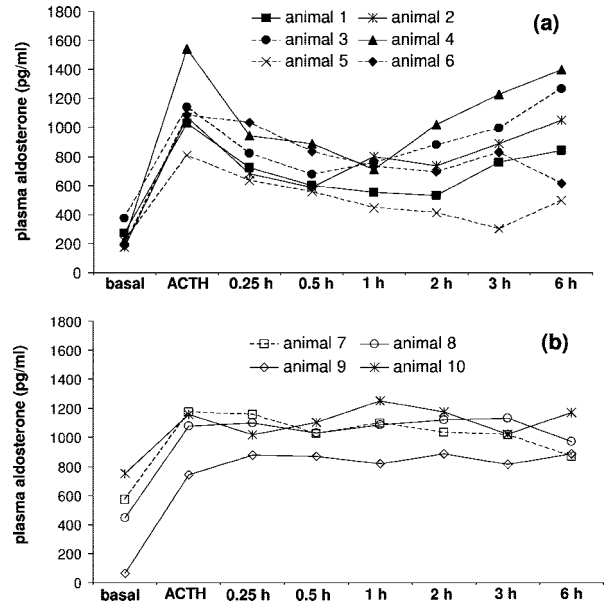

Figure 3. Lowering of aldosterone plasma levels in vivo of (a) the compound **21** treated group (animals 1−6) and (b) the vehicle treated group (animals 7−10). Shown are the aldosterone plasma levels of the individual animals predose before sc application of 1 mg/kg ACTH, and before iv application of 20 mg/kg **21** (animals 1−6) or vehicle (animals 7−10), followed by sampling 0.25, 0.5, 1, 2, 3, and 6 h postdose.

is significantly lower in the case of the dihydro-1*H*-quinolin-2-ones with IC_{50} values in the micromolar range. The investigated molecules reach the circulation after peroral administration to rats (e.g., **12** with a peroral bioavailability of 71%). Moreover, it has been found that isoquinoline derivative **21** significantly reduces the plasma aldosterone levels of ACTH stimulated rats. Our current research focuses on further in vivo investigations of compound **21** and structurally related compounds in disease oriented models to determine their capability to prevent or reverse myocardial fibrosis and reduce CHF induced mortality.

Experimental Section

Chemical and Analytical Methods. Melting points were measured on a Mettler FP1 melting point apparatus and are uncorrected. ^{1}H NMR and ^{13}C spectra were recorded on a Bruker DRX-500 instrument. Chemical shifts are given in parts per million (ppm), and tetramethylsilane (TMS) was used as internal standard for spectra obtained in DMSO-d_6 and $CDCl_3$. All coupling constants (*J*) are given in hertz. Mass spectra (LC/MS) were measured on a TSQ Quantum (Thermo Electron Corporation) instrument with a RP18 100-3 column (Macherey Nagel) and with water/acetonitrile mixtures as eluents. GC/MS spectra were measured on a GCD Series G1800A (Hewlett-Packard) instrument with an Optima-5-MS (0.25 μM, 30 m) column (Macherey Nagel). Elemental analyses were carried out at the Department of Chemistry, University of Saarbrücken. Reagents were used as obtained from commercial suppliers without further purification. Solvents were distilled before use. Dry solvents were obtained by distillation from appropriate drying reagents and stored over molecular sieves. Flash chromatography was performed on silica gel 40 (35/40−63/70 μM) with petroleum ether/ethyl acetate mixtures as eluents, and the reaction progress was determined by thin-layer chromatography analyses on Alugram SIL G/UV254 (Macherey Nagel). Visualization was accomplished with UV light and $KMnO_4$ solution. All microwave irradiation experiments were carried out in a CEM-Discover monomode microwave apparatus.

The following compounds were prepared according to previously described procedures: 6-bromo-1,2,3,4-tetrahydronaphthalen-2-ol

(**2a**),[21] 6-bromo-3,4-dihydroquinolin-2(1*H*)-one (**12a**),[24] 5-bromo-1,3-dihydro-2*H*-indol-2-one (**13a**),[25] 6-bromo-8-nitro-3,4-dihydroquinolin-2(1*H*)-one (**18a**).[27]

Synthesis of the Target Compounds. Procedure A.[17] Boronic acid (0.75 mmol, 1 equiv), aryl bromide or -triflate (0.9−1.3 equiv), and tetrakis(triphenylphosphane)palladium(0) (43 mg, 37.5 μmol, 5 mol %) were suspended in 1.5 mL DMF in a 10 mL septum-capped tube containing a stirring magnet. To this was added a solution of $NaHCO_3$ (189 mg, 2.25 mmol, 3 equiv) in 1.5 mL water and the vial was sealed with an Teflon cap. The mixture was irradiated with microwaves for 15 min at a temperature of 150 °C with an initial irradiation power of 100 W. After the reaction, the vial was cooled to 40 °C, the crude mixture was partitioned between ethyl acetate and water and the aqueous layer was extracted three times with ethyl acetate. The combined organic layers were dried over $MgSO_4$ and the solvents were removed in vacuo. The coupling products were obtained after flash chromatography on silica gel (petroleum ether/ethyl acetate mixtures) and/or crystallization.

Procedure B. Boronic acid (1 equivalent), aryl bromide or (1.3−1.5 equiv), and tetrakis(triphenylphosphane)palladium(0) (5 mol%) were suspended in toluene/ethanol 4/1 to give a 0.07−0.1 M solution of boronic acid under an atmosphere of nitrogen. To this was added a 1 N aqueous solution of Na_2CO_3 (6 equivalents). The mixture was then refluxed for 12−18 h, cooled to room temperature, diluted with water, and extracted several times with ethyl acetate. The combined extracts were dried over $MgSO_4$, concentrated, and purified by flash chromatography on silica gel (petroleum ether/ethyl acetate mixtures) and/or crystallization.

3-(5,6,7,8-Tetrahydronaphthalen-2-yl)pyridine (1). Compound **1** was obtained according to procedure A from **1a** (280 mg, 1.0 mmol) and 3-pyridineboronic acid (160 mg, 1.3 mmol) after flash chromatography on silica gel (petroleum ether/ethyl acetate, 2/1, $R_f = 0.20$) as a pale yellow oil (142 mg, 0.68 mmol, 68%), mp (HCl salt) 200−202 °C. LC/MS *m/z* 210.27 (MH^+). Anal. ($C_{15}H_{15}N \cdot HCl$) C, H, N.

6-Pyridin-3-yl-1,2,3,4-tetrahydronaphthalen-2-ol (2). Compound **2** was obtained according to procedure A from **2a** (114 mg, 0.50 mmol) and 3-pyridineboronic acid (80 mg, 0.65 mmol) after flash chromatography on silica gel (ethyl acetate, $R_f = 0.27$) as a colorless solid (96 mg, 0.43 mmol, 86%), mp 118−120 °C. LC/MS *m/z* 226.23 (MH^+). Anal. ($C_{15}H_{15}NO \cdot 0.1H_2O$) C, H, N.

3-(6-Methoxy-5,6,7,8-tetrahydronaphthalen-2-yl)pyridine (3). To a suspension of NaH (73 mg, 1.84 mmol, 60% dispersion in oil) in 10 mL dry THF was added dropwise a solution of **2** (345 mg, 1.53 mmol) in 5 mL THF at room temperature. The mixture was heated to 50 °C until evolution of hydrogen ceased and then cooled to room temperature again. Thereupon, a solution of methyl iodide (326 mg, 2.30 mmol) in 5 mL THF was added via canula and stirring was continued at 50 °C for 3 h. The mixture was treated with saturated aqueous NH_4Cl solution and extracted three times with ethyl acetate. The combined organic extracts were washed with water and brine, dried over $MgSO_4$, and evaporated to dryness. The crude product was purified by flash chromatography on silica gel (petroleum ether/ethyl acetate, 7/3, $R_f = 0.09$) to afford **3** as a colorless oil (289 mg, 1.21 mmol, 79%), mp (HCl salt) 188−190 °C. LC/MS *m/z* 240.29 (MH^+). Anal. ($C_{16}H_{17}NO \cdot HCl \cdot 0.6H_2O$) C, H, N.

3-(6-Ethoxy-5,6,7,8-tetrahydronaphthalen-2-yl)pyridine (4). Compound **4** was obtained as described for **3** starting from **2** (270 mg, 1.20 mmol), NaH (58 mg, 1.44 mmol, 60% dispersion in oil), and ethyl bromide (196 mg, 1.80 mmol) after flash chromatography on silica gel (petroleum ether/ethyl acetate, 1/1, $R_f = 0.31$) as a colorless oil (198 mg, 0.78 mmol, 65%), mp (HCl salt) 186−188 °C. LC/MS *m/z* 254.29 (MH^+). Anal. ($C_{17}H_{19}NO \cdot HCl \cdot 0.5H_2O$) C, H, N.

6-Pyridin-3-yl-1,2,3,4-tetrahydronaphthalene-2-carbonitrile (5). Compound **5** was obtained according to procedure A from **5a** (130 mg, 0.55 mmol) and 3-pyridineboronic acid (88 mg, 0.72 mmol) after flash chromatography on silica gel (petroleum ether/ethyl acetate, 1/1, $R_f = 0.17$) as a colorless solid (91 mg, 0.39 mmol, 71%), mp 110−111 °C. ^{1}H NMR (500 MHz, $CDCl_3$): δ = 2.12 (m, 1H), 2.23 (m, 1H), 2.92 (m, 1H), 3.02−3.13 (m, 3H), 3.18 (dd, ^2J = 16.4 Hz, ^3J = 5.7 Hz, 1H), 7.19 (d, ^3J = 7.9 Hz, 1H), 7.31 (s, 1H), 7.33−7.37 (m, 2H), 7.83 (m, 1H), 8.57 (dd, ^3J = 5.0 Hz, ^4J = 1.6 Hz, 1H), 8.80 (d, ^4J = 1.6 Hz, 1H). ^{13}C NMR (125 MHz, $CDCl_3$): δ 25.5, 26.1, 27.1, 32.1, 121.8, 123.5, 125.1, 127.8, 129.8, 132.3, 134.2, 135.5, 136.2, 136.4, 148.2, 148.5. LC/MS *m/z* 235.26 (MH^+). Anal. ($C_{16}H_{14}N_2 \cdot 0.1H_2O$) C, H, N.

6-Pyridin-3-yl-3,4-dihydronaphthalene-2-carbonitrile (6). To a solution of **6a** (562 mg, 1.58 mmol) in 10 mL degassed DMF were added zinc cyanide (117 mg, 1.00 mmol) and tetrakis(triphenylphosphane)palladium(0) (173 mg, 0.15 mmol) and the mixture was heated at 100 °C for 2 h. After cooling to room temperature, the mixture was diluted with 200 mL of water and extracted three times with ethyl acetate. The combined organic extracts were washed with water and brine, dried over $MgSO_4$, and evaporated to dryness. The crude product was crystallized from petroleum ether/ethyl acetate to afford **6** as colorless needles (286 mg, 1.23 mol, 78%), mp 142−143 °C. LC/MS *m/z* 233.23 (MH^+). Anal. ($C_{16}H_{12}N_2$) C, H, N.

4-Methyl-7-pyridin-3-yl-3,4-dihydro-2*H*-1,4-benzoxazine (7). Compound **7** was obtained according to procedure A from 7-bromo-4-methyl-3,4-dihydro-2*H*-1,4-benzoxazine (228 mg, 1.00 mmol) and 3-pyridineboronic acid (160 mg, 1.30 mmol) after flash chromatography on silica gel (petroleum ether/ethyl acetate, 1/1, $R_f = 0.26$) as an off-white solid (102 mg, 0.45 mmol, 45%), mp 70−72 °C. LC/MS *m/z* 227.21 (MH^+). Anal. ($C_{14}H_{14}N_2O$) C, H, N.

3-(2,3-Dihydro-1,4-benzodioxin-6-yl)pyridine (8). Compound **8** was obtained according to procedure A from 6-bromo-2,3-dihydro-1,4-benzodioxine (215 mg, 1.00 mmol) and 3-pyridineboronic acid (160 mg, 1.30 mmol) after flash chromatography on silica gel (petroleum ether/ethyl acetate, 7/3, $R_f = 0.14$) as a colorless solid (184 mg, 0.86 mmol, 86%), mp 59−61 °C. LC/MS *m/z* 214.19 (MH^+). Anal. ($C_{16}H_{12}N_2$) C, H, N.

6-Pyridin-3-yl-3,4-dihydronaphthalen-2(1*H*)-one (9). Compound **9** was obtained according to procedure A from 6-bromo-2-tetralone (113 mg, 0.50 mmol) and 3-pyridineboronic acid (80 mg, 0.65 mmol) after flash chromatography on silica gel (petroleum ether/ethyl acetate, 1/1, $R_f = 0.15$) as a colorless oil (97 mg, 0.43 mmol, 86%), mp (HCl salt) 180−182 °C. LC/MS *m/z* 224.20 (MH^+). Anal. ($C_{15}H_{13}NO \cdot HCl \cdot 0.4H_2O$) C, H, N.

5-Pyridin-3-yl-2,3-dihydro-1*H*-inden-1-one (10). Compound **10** was obtained according to procedure A from 5-bromo-1-indanone (211 mg, 1.00 mmol) and 3-pyridineboronic acid (160 mg, 1.30 mmol) after flash chromatography on silica gel (petroleum ether/ethyl acetate, 1/1, $R_f = 0.14$) as a colorless solid (146 mg, 0.69 mmol, 69%), mp 122−123 °C. LC/MS *m/z* 210.69 (MH^+). Anal. ($C_{14}H_{11}NO \cdot 0.1H_2O$) C, H, N.

6-(5-Methoxypyridin-3-yl)-3,4-dihydronaphthalen-2(1*H*)-one (11). **11** was obtained according to procedure A from 6-bromo-2-tetralone (225 mg, 1.00 mmol) and 5-methoxy-3-pyridineboronic acid (199 mg, 1.30 mmol) after flash chromatography on silica gel (petroleum ether/ethyl acetate, 1/1, $R_f = 0.15$) as an off-white solid (133 mg, 0.53 mmol, 53%), mp 109−110 °C. LC/MS *m/z* 254.01 (MH^+). Anal. ($C_{16}H_{15}NO_2$) C, H, N.

6-Pyridin-3-yl-3,4-dihydroquinolin-2(1*H*)-one (12). Compound **12** was obtained according to procedure B from **12a** (2.71 g, 12.0 mmol) and 3-pyridineboronic acid (1.23 g, 10.0 mmol) after crystallization from acetone/diethyl ether as colorless needles (2.15 g, 9.59 mmol, 96%), mp 181−183 °C. ^{1}H NMR (500 MHz, DMSO-d_6): δ 2.49 (t, ^3J = 7.3 Hz, 2H), 2.95 (t, ^3J = 7.3 Hz, 2H), 6.95 (d, ^3J = 8.2 Hz, 1H), 7.43 (ddd, ^3J = 7.9 Hz, ^3J = 4.7 Hz, ^5J = 0.6 Hz, 1H), 7.51 (dd, ^3J = 8.2 Hz, ^4J = 2.2 Hz, 1H), 7.56 (d, ^4J = 2.1 Hz, 1H), 8.00 (ddd, ^3J = 7.9 Hz, ^4J = 2.2 Hz, ^4J = 1.6 Hz, 1H), 8.50 (dd, ^3J = 4.7 Hz, ^4J = 1.5 Hz, 1H), 8.84 (d, ^4J = 2.2 Hz, 1H), 10.19 (s, 1H). ^{13}C NMR (125 MHz, DMSO-d_6): δ = 24.8, 30.3, 115.6, 123.8, 124.3, 125.6, 126.2, 130.6, 133.4, 135.2, 138.4, 147.2, 147.8, 170.2. LC/MS *m/z* 225.25 (MH^+). Anal. ($C_{14}H_{12}N_2O \cdot 0.1H_2O$) C, H, N.

5-Pyridin-3-yl-1,3-dihydro-2*H*-indol-2-one (13). Compound **13** was obtained according to procedure A from **13a** (159 mg, 0.75 mmol) and 3-pyridineboronic acid (123 mg, 1.00 mmol) after crystallization

from acetone/diethyl ether as colorless needles (129 mg, 0.61 mmol, 81%), mp 218−220 °C. LC/MS *m/z* 211.01 (MH^+). Anal. ($C_{13}H_{10}N_2O \cdot 0.3H_2O$) C, H, N.

1-Methyl-6-pyridin-3-yl-3,4-dihydroquinolin-2(1*H*)-one (14). Compound **14** was obtained according to procedure A from **14a** (110 mg, 0.46 mmol) and 3-pyridineboronic acid (74 mg, 0.60 mmol) after flash chromatography on silica gel (petroleum ether/ethyl acetate, 2/3, $R_f = 0.07$) as colorless needles (83 mg, 0.35 mmol, 76%), mp 100−101 °C. LC/MS *m/z* 239.80. Anal. ($C_{15}H_{14}N_2O \cdot 0.1H_2O$) C, H, N.

1-Ethyl-6-pyridin-3-yl-3,4-dihydroquinolin-2(1*H*)-one (15). Compound **15** was obtained according to procedure A from **15a** (229 mg, 0.90 mmol) and 3-pyridineboronic acid (92 mg, 0.75 mmol) after flash chromatography on silica gel (petroleum ether/ethyl acetate, 1/1, $R_f = 0.09$) and crystallization from acetone/diethyl ether as colorless plates (125 mg, 0.50 mmol, 55%), mp 91−92 °C. LC/MS *m/z* 253.00 (MH^+). Anal. ($C_{16}H_{16}N_2O \cdot 0.1H_2O$) C, H, N.

1-(1-Methylethyl)-6-pyridin-3-yl-3,4-dihydroquinolin-2(1*H*)-one (16). Compound **16** was obtained according to procedure A from **16a** (174 mg, 0.65 mmol) and 3-pyridineboronic acid (74 mg, 0.60 mmol) after flash chromatography on silica gel (petroleum ether/ethyl acetate, 1/1, $R_f = 0.14$) as a colorless solid (47 mg, 0.18 mmol, 29%), mp 100−101 °C. LC/MS *m/z* 267.10 (MH^+). Anal. ($C_{17}H_{18}N_2O$) C, H, N.

8-Chloro-6-pyridin-3-yl-3,4-dihydroquinolin-2(1*H*)-one (17). To a solution of **12** (560 mg, 2.50 mmol) in 5 mL DMF was added *N*-chlorosuccinimide (368 mg, 2.75 mmol) in 5 mL DMF over a period of 2 h at 65 °C. After additional 3 h at 65 °C, the mixture was poured into ice water and extracted three times with ethyl acetate. The combined organic layers were washed with water and brine, dried over $MgSO_4$, and the solvent was evaporated in vacuo. **17** was obtained after flash chromatography on silica gel (petroleum ether/ethyl acetate, 3/7, $R_f = 0.15$) and crystallization from acetone/diethyl ether as colorless needles (225 mg, 0.87 mmol, 35%), mp 177−178 °C. GC/MS *m/z* 258.95 (M^+). Anal. ($C_{14}H_{11}ClN_2O \cdot 0.1H_2O$) C, H, N.

8-Nitro-6-pyridin-3-yl-3,4-dihydroquinolin-2(1*H*)-one (18). Compound **18** was obtained according to procedure B from **18a** (1.0 g, 3.70 mmol) and 3-pyridineboronic acid (546 mg, 4.44 mmol) after flash chromatography on silica gel (ethyl acetate, $R_f = 0.15$) as yellow needles (311 mg, 1.16 mmol, 31%), mp 187−189 °C. LC/MS *m/z* 269.94 (MH^+). Anal. ($C_{14}H_{11}N_3O_3$) C, H, N.

6-(5-Methoxypyridin-3-yl)-3,4-dihydroquinolin-2(1*H*)-one (19). Compound **19** was obtained according to procedure A from **12a** (170 mg, 0.75 mmol) and 5-methoxy-3-pyridineboronic acid (150 mg, 0.98 mmol) after crystallization from acetone/diethyl ether as colorless needles (77 mg, 0.30 mmol, 40%), mp 213−215 °C. LC/MS *m/z* 255.02 (MH^+). Anal. ($C_{15}H_{14}N_2O_2$) C, H, N.

6-(5-methoxypyridin-3-yl)-1-methyl-3,4-dihydroquinolin-2(1*H*)-one (20). Compound **20** was obtained according to procedure A from **14a** (200 mg, 0.83 mmol) and 5-methoxy-3-pyridineboronic acid (115 g, 0.75 mmol) after crystallization from acetone/diethyl ether as colorless needles (132 mg, 0.49 mmol, 66%), mp 158−159 °C. LC/MS *m/z* 268.95 (MH^+). Anal. ($C_{16}H_{16}N_2O_2 \cdot 0.1H_2O$) C, H, N.

6-Isoquinolin-4-yl-3,4-dihydroquinolin-2(1*H*)-one (21). Compound **21** was obtained according to procedure B from **12a** (1.55 g, 6.85 mmol) and 4-isoquinolineboronic acid (950 mg, 5.50 mmol) after crystallization from acetone/diethyl ether as colorless needles (800 mg, 2.92 mmol, 53%), mp 221−222 °C. LC/MS *m/z* 275.04 (MH^+). Anal. ($C_{18}H_{14}N_2O \cdot 0.1H_2O$) C, H: calcd, 5.18, found, 5.60, N.

6-Isoquinolin-4-yl-1-methyl-3,4-dihydroquinolin-2(1*H*)-one (22). Compound **22** was obtained according to procedure A from **14a** (264 mg, 1.10 mmol) and 4-isoquinolineboronic acid (172 mg, 1.00 mmol) after crystallization from acetone/diethyl ether as colorless needles (163 mg, 0.57 mmol, 57%), mp 175−176 °C. LC/MS *m/z* 289.91 (MH^+). Anal. ($C_{19}H_{16}N_2O$) C, H, N.

6-Pyrimidin-5-yl-3,4-dihydroquinolin-2(1*H*)-one (23). Compound **23** was obtained according to procedure A from **12a** (226 mg, 1.00 mmol) and 5-pyrimidineboronic acid (103 mg, 0.83 mmol) after crystallization from ethanol as colorless needles (75 mg, 0.33 mmol, 40%), mp 232−233 °C. LC/MS *m/z* 225.74 (MH^+). Anal. ($C_{13}H_{11}N_3O \cdot 0.2H_2O$) C, H, N.

6-Pyridin-3-yl-3,4-dihydroquinoline-2(1*H*)-thione (24). Compound **24** A suspension of **12** (395 mg, 1.76 mmol) and Lawesson's reagent (356 mg, 0.88 mmol) in dry toluene was refluxed for 30 min under an atmosphere of nitrogen. After cooling to room temperature, the solvent was removed in vacuo and the residue was purified by flash chromatography on silica gel (petroleum ether/ethyl acetate, 3/7, $R_f = 0.31$) to afford **24** as yellow plates (63 mg, 0.26 mmol, 15%), mp 265−267 °C. LC/MS *m/z* 241.05 (MH^+). Anal. ($C_{14}H_{12}N_2S$) C, H, N.

8-Chloro-6-pyridin-3-yl-3,4-dihydroquinoline-2(1*H*)-thione (25). Compound **25** was obtained as described for **24** starting from **17** (900 mg, 3.48 mmol) and Lawesson's reagent (985 mg, 2.44 mmol) after flash chromatography on silica gel (ethyl acetate, $R_f = 0.26$) and crystallization from acetone/diethyl ether as yellow needles (212 mg, 0.77 mmol, 22%), mp 174−175 °C. GC/MS *m/z* 273.95 ($M^{35}Cl^+$), 275.95 ($M^{37}Cl^+$). Anal. ($C_{14}H_{11}ClN_2S$) C, H, N.

7-Pyridin-3-yl-2*H*-1,4-benzothiazin-3(4*H*)-one (26). Compound **26** was obtained according to general procedure B from 7-bromo-2*H*-1,4-benzothiazin-3(4*H*)-one (1.15 g, 4.71 mmol) and 3-pyridineboronic acid (695 mg, 5.56 mmol) after flash chromatography on silica gel (petroleum ether/ethyl acetate, 1/1, $R_f = 0.20$) and crystallization from ethanol as colorless needles (486 mg, 2.01 mmol, 43%), mp 238−240 °C. LC/MS *m/z* 242.99 (MH^+). Anal. ($C_{13}H_{10}N_2OS \cdot 0.2H_2O$) C, H, N.

Biological Methods. 1. Enzyme Preparations. CYP17 and CYP19 preparations were obtained by described methods: the 50000*g* sediment of *E. coli* expressing human CYP17[32] and microsomes from human placenta for CYP19.[34]

2. Enzyme Assays. The following enzyme assays were performed as previously described: CY17[32] and CYP19.[34]

3. Activity and Selectivity Assay Using V79 Cells. V79 MZh 11B1 and V79 MZh 11B2 cells[10,28] were incubated with [4-^{14}C]-11-deoxycorticosterone as substrate and inhibitor in at least three different concentrations. The enzyme reactions were stopped by addition of ethyl acetate. After vigorous shaking and a centrifugation step (10000*g*, 2 min), the steroids were extracted into the organic phase, which was then separated. The conversion of the substrate was analyzed by HPTLC and a phosphoimaging system as described.

4. Inhibition of Human Hepatic CYP Enzymes. The recombinantly expressed enzymes from baculovirus-infected insect microsomes (Supersomes) were used and the manufacturer's instructions (www.gentest.com) were followed.

5. In Vivo Pharmacokinetics. Animal trials were conducted in accordance with institutional and international ethical guidelines for the use of laboratory animals. Cassette dosing: Male Wistar rats weighing 297−322 g (Janvier, France) were housed in a temperature-controlled room (20−24 °C) and maintained in a 12 h light/12 h dark cycle. Food and water were available ad libitum. The animals were anaesthetized with a ketamine (135 mg/kg)/xylazine (10 mg/kg) mixture and cannulated with silicone tubing via the right jugular vein. Prior to the first blood sampling, animals were connected to a counterbalanced system and tubing to perform blood sampling in the freely moving rat. Separate stock solutions (5 mg/mL) were prepared for the tested compounds in labrasol/water (1:1; v/v), leading to a clear solution. Immediately before application, the cassette dosing mixture was prepared by adding equal volumes of the stock solutions to end up with a final concentration of 1 mg/mL for each compound. The mixture was applied perorally to 3 rats with an injection volume of 5 mL/kg (Time 0). Blood samples (250 μL) were collected 1 h before application and 1, 2, 4, 6, 8, and 24 h thereafter. They were centrifuged at 650*g* for 10 min at 4 °C and then the plasma was harvested and kept at −20 °C until LC/MS analysis. To 50 μL of rat plasma sample and calibration standard 100 μL of acetonitrile containing the internal standard was added. Samples and standards were vigorously shaken and centrifuged for 10 min at 6000*g* and

20 °C. For the test items, an additional dilution was performed by mixing 50 μL of the particle free supernatant with 50 μL water. An aliquot was transferred to 200 μL sampler vials and subsequently subjected to LC-MS/MS. HPLC-MS/MS analysis and quantification of the samples was carried out on a Surveyor-HPLC-system coupled with a TSQ Quantum (ThermoFinnigan) triple quadrupole mass spectrometer equipped with an electrospray interface (ESI). The mean of absolute plasma concentrations (±SEM) was calculated for the three rats, and the regression was performed on group mean values. The pharmacokinetic analysis was performed using a noncompartment model (PK Solutions 2.0, Summit Research Services). Single dosing: the single dose experiments were performed as described for the cassette dosing procedure with male Wistar rats weighing 234−276 g (Janvier, France). Separate stock solutions (5 mg/mL) were prepared for compound **12** in PEG400/water/ethanol (50:40:10; v/v/v) and for compound **21** in labrasol/water (1:1; v/v), leading to clear solutions. Compound **12** was applied at 25 mg/kg perorally and 1 mg/kg intravenously and compound **21** at 25 mg/kg perorally to 4 rats each. Additional blood samples were taken 10 and 12 h after application in case of peroral application and 0.08, 0.25, 0.50, and 0.75 h in case of intravenous application of compound **12**, respectively.

6. Plasma Protein Binding. A 10 mM test compound solution and ketoprofen solution is prepared in acetonitrile. The test compound solution is diluted with solvent to the 50 fold concentration (150 μM, working solution) used in the assay (3 μM). In a 1.5 mL Eppendorf vial, 3 μL of working solution are given to 147 μL of serum (rat or human) and mixed. For recovery, the same dilutions are done in ultrafiltrated serum. The solutions are incubated for 1 h at 37 °C. The whole samples (6 test solutions, 6 recovery samples) are centrifuged at 8000*g* for 20 min using Centrifree micropartition devices (Millipore). The 75 μL of ultrafiltrate (UF) sample is removed for sample preparation. To 75 μL of sample or 150 μL calibration standard, 75 or 150 μL acetonitrile containing the internal standard (ketoprofen, 1 μM) is added to precipitate plasma proteins. Samples are then vigorously shaken (10 s) and centrifuged for 10 min at 6000*g* and 20 °C. An aliquot (70 μL) of the particle-free supernatant is subsequently subjected to LC-MS/MS. The degree of binding to the plasma proteins (PPB) is calculated by the following equation: % Protein binding = $(1 - [\text{ligand}_{\text{ultrafiltrate}}]/[\text{ligand}_{\text{total}}]) \cdot 100$.

7. Cytotoxicity. Cell viability upon drug exposure was determined using a fluorimetric alamar blue conversion assay using a 96-well plate format. Briefly, U-937 cells (human monocytic leukemia) were seeded in growth medium into 96-well plates at a final density of 5×10^4 cells/mL and exposed to the respective compounds for the indicated time intervals (six replicates per concentration). At the end of the exposure time, alamar blue (Biosource International, Camarillo, CA) was added at 10% (v/v) and incubated for 4 h. Fluorescence intensity was quantitated using a Wallac Victor fluorescence plate reader (Perkin-Elmer, Wellesley, MA) at 530 nm excitation and 590 nm emission. Relative viability of cells was determined in relation to the untreated control. Control wells containing compound only were included to detect potential interference of the compound with the indicator system. Also, media only controls were included to account for background fluorescence. Viability of cells prior to cytotoxicity experiments was determine by Trypan Blue staining. Cells were diluted 1:3 in 0.4% (w/v) Trypan Blue (Sigma), and counted in a hemacytomer.

Acknowledgment. The assistance in performing the in vitro tests by Gertrud Schmitt and Jeannine Jung is highly appreciated. We would also like to acknowledge the undergraduate research participants Judith Horzel, Helena Rübel, and Thomas Jakoby whose work contributed to the presented results. S.L. is grateful to Saarland University for a scholarship (Landesgraduierten-Förderung). Thanks are due to Prof. J. J. Rob Hermans, University of Maastricht, The Netherlands, for supplying the V79 CYP11B1 cells, and Prof. Rita Bernhardt, Saarland University, for supplying the V79 CYP11B2 cells. The determination of the cyctotoxicity by Dr. Reiner Class, Pharmacelsus CRO, Saarbrücken, as well as the investigation of the hepatic CYP profile by Dr. Ursula Müller-Vieira, Pharmacelsus CRO, is gratefully acknowledged.

Supporting Information Available: Aldosterone concentrations in the individual animals at all sampling points, NMR spectroscopic data of the target compounds **1**−**4**, **6**−**11**, **13**−**26**, full experimental details, and spectroscopic characterization of the reaction intermediates **1a**, **5a**, **5b**, **6a**, **14a**−**16a**, elemental analysis results of compounds **1**−**26**. This material is available free of charge via the Internet at http://pubs.acs.org.

References

(1) Weber, K. T. Aldosterone in congestive heart failure. *N. Engl. J. Med.* **2001**, *345*, 1689−1697.

(2) (a) Brilla, C. G. Renin-angiotensin-aldosterone system and myocardial fibrosis. *Cardiovasc. Res.* **2000**, *47*, 1–3. (b) Lijnen, P.; Petrov, V. Induction of cardiac fibrosis by aldosterone. *J. Mol. Cell. Cardiol* **2000**, *32*, 865–879.

(3) Satoh, M.; Nakamura, M.; Saitoh, H.; Satoh, H.; Akatsu, T.; Iwasaka, J.; Masuda, T.; Hiramori, K. Aldosterone synthase (CYP11B2) expression and myocardial fibrosis in the failing human heart. *Clin. Sci.* **2002**, *102*, 381–386.

(4) (a) Pitt, B.; Zannad, F.; Remme, W. J.; Cody, R.; Castaigne, A.; Perez, A.; Palensky, J.; Wittes, J. The effect of spironolactone on morbidity and mortality in patients with severe heart failure. *N. Engl. J. Med.* **1999**, *341*, 709–717. (b) Pitt, B.; Remme, W.; Zannad, F.; Neaton, J.; Martinez, F.; Roniker, B.; Bittman, R.; Hurley, S.; Kleiman, J.; Gatlin, M. Eplerenone, a selective aldosterone blocker, in patients with left ventricular dysfunction after myocardial infarction. *N. Engl. J. Med.* **2003**, *348*, 1309–1321.

(5) Izawa, H.; Murohara, T.; Nagata, K.; Isobe, S.; Asano, H.; Amano, T.; Ichihara, S.; Kato, T.; Ohshima, S.; Murase, Y.; Iino, S.; Obata, K.; Noda, A.; Okumura, K.; Yokota, M. Mineralocorticoid receptor antagonism ameliorates left ventricular diastolic dysfunction and myocardial fibrosis in mildly symptomatic patients with idiopathic dilated cardiomyopathy: a pilot study. *Circulation* **2005**, *112*, 2940–2945.

(6) Juurlink, D. N.; Mamdani, M. M.; Lee, D. S.; Kopp, A.; Austin, P. C.; Laupacis, A.; Redelmeier, D. A. Rates of hyperkalemia after publication of the Randomized Aldactone Evaluation Study. *N. Engl. J. Med.* **2004**, *351*, 543–551.

(7) Delcayre, C.; Swynghedauw, B. Molecular mechanisms of myocardial remodeling. The role of aldosterone. *J. Mol. Cell. Cardiol.* **2002**, *34*, 1577–1584.

(8) (a) Wehling, M. Specific, nongenomic actions of steroid hormones. *Annu. Rev. Physiol.* **1997**, *59*, 365–393. (b) Lösel, R.; Wehling, M. Nongenomic actions of steroid hormones. *Nat. Rev. Mol. Cell. Biol.* **2003**, *4*, 46–55.

(9) Hartmann, R. W. Selective inhibition of steroidogenic P450 enzymes: Current status and future perspectives. *Eur. J. Pharm. Sci* **1994**, *2*, 15–16.

(10) Ehmer, P. B.; Bureik, M.; Bernhardt, R.; Müller, U.; Hartmann, R. W. Development of a test system for inhibitors of human aldosterone synthase (CYP11B2): Screening in fission yeast and evaluation of selectivity in V79 cells. *J. Steroid Biochem. Mol. Biol.* **2002**, *81*, 173–179.

(11) Kawamoto, T.; Mitsuuchi, Y.; Toda, K.; Yokoyama, Y.; Miyahara, K.; Miura, S.; Ohnishi, T.; Ichikawa, Y.; Nakao, K.; Imura, H.; Ulick, S.; Shizuta, Y. Role of steroid 11β-hydroxylase and steroid 18-hydroxylase in the biosynthesis of glucocorticoids and mineralocorticoids in humans. *Proc. Natl. Acad. Sci. U.S.A.* **1992**, *89*, 1458–1462.

(12) Ulmschneider, S.; Müller-Vieira, U.; Mitrenga, M.; Hartmann, R. W.; Oberwinkler-Marchais, S.; Klein, C. D.; Bureik, M.; Bernhardt, R.; Antes, I.; Lengauer, T. Synthesis and evaluation of imidazolylmethylenetetrahydronaphthalenes and imidazolylmethyleneindanes: Potent inhibitors of aldosterone synthase. *J. Med. Chem.* **2005**, *48*, 1796–1805.

(13) Ulmschneider, S.; Müller-Vieira, U.; Klein, C. D.; Antes, I.; Lengauer, T.; Hartmann, R. W. Synthesis and evaluation of (pyridylmethylene-)tetrahydronaphthalenes/-indanes and structurally modified derivatives: Potent and selective inhibitors of aldosterone synthase. *J. Med. Chem.* **2005**, *48*, 1563–1575.

(14) Voets, M.; Antes, I.; Scherer, C.; Müller-Vieira, U.; Biemel, K.; Barassin, C.; Oberwinkler-Marchais, S.; Hartmann, R. W. Heteroaryl substituted naphthalenes and structurally modified derivatives: Selective inhibitors of CYP11B2 for the treatment of congestive heart failure and myocardial fibrosis. *J. Med. Chem.* **2005**, *48*, 6632–6642.

(15) Lucas, S.; Heim, R.; Negri, M.; Antes, I.; Ries, C.; Schewe, K. E.; Bisi, A.; Gobbi, S.; Hartmann, R. W. Novel aldosterone synthase inhibitors with extended carbocyclic skeleton by a combined ligand-based and structure-based drug design approach. *J. Med. Chem.* **2008**, *51*, 6138–6149.

(16) Voets, M.; Antes, I.; Scherer, C.; Müller-Vieira, U.; Biemel, K.; Oberwinkler-Marchais, S.; Hartmann, R. W. Synthesis and evaluation of heteroaryl-substituted dihydronaphthalenes and indenes: Potent and selective inhibitors of aldosterone synthase (CYP11B2) for the treatment of congestive heart failure and myocardial fibrosis. *J. Med. Chem.* **2006**, *49*, 2222–2231.

(17) Appukkuttan, P.; Orts, A. B.; Chandran, R., P.; Goeman, J. L.; van der Eycken, J.; Dehaen, W.; van der Eycken, E. Generation of a small library of highly electron-rich 2-(hetero)aryl-substituted phenethylamines by the Suzuki−Miyaura reaction: A short synthesis of an apogalanthamine analogue. *Eur. J. Org. Chem.* **2004**, 3277–3285.

(18) Bengtson, A.; Hallberg, A.; Larhed, M. Fast synthesis of aryl triflates with controlled microwave heating. *Org. Lett.* **2002**, *4*, 1231–1233.

(19) Carreñño, M. C.; García-Cerrada, S.; Urbano, A. From central to helical chirality: Synthesis of P and M enantiomers of [5]helicenequinones and bisquinones from (*SS*)-2-(*p*-tolylsulfinyl)-1,4-benzoquinone. *Chem. Eur. J.* **2003**, *9*, 4118–4131.

(20) Selnick, H. G.; Smith, G. R.; Tebben, A. J. An improved procedure for the cyanation of aryl triflates: A convenient synthesis of 6-cyano-1,2,3,4-tetrahydroisoquinoline. *Synth. Commun.* **1995**, *25*, 3255–3261.

(21) Tschaen, D. M.; Abramson, L.; Cai, D.; Desmond, R.; Dolling, U.-H.; Frey, L.; Karady, S.; Shi, Y.-J.; Verhoeven, T. R. Asymmetric Synthesis of MK-0499. *J. Org. Chem.* **1995**, *60*, 4324–4330.

(22) Mewshaw, R. E.; Edsall, R. J., Jr.; Yang, C.; Manas, E. S.; Xu, Z. B.; Henderson, R. A.; Keith, J. C., Jr.; Harris, H. A. ERβ ligands. 3. Exploiting two binding orientations of the 2-phenylnaphthalene scaffold to achieve ERβ selectivity. *J. Med. Chem.* **2005**, *48*, 3953–3979.

(23) DeBernardis, J. F.; Kerkman, D. J.; Winn, M.; Bush, E. N.; Arendsen, D. L.; McClellan, W. J.; Kyncl, J. J.; Basha, F. Z. Conformationally defined adrenergic agents. 1. Design and synthesis of novel α_2 selective adrenergic agents: Electrostatic repulsion based conformational prototypes. *J. Med. Chem.* **1985**, *28*, 1319–1404.

(24) Occhiato, E. G.; Ferrali, A.; Menchi, G.; Guarna, A.; Danza, G.; Comerci, A.; Mancina, R.; Serio, M.; Garotta, G.; Cavalli, A.; De Vivo, M.; Recanatini, M. Synthesis, biological activity, and three-dimensional quantitative structure-activity relationship model for a series of benzo[*c*]quinolizin-3-ones, nonsteroidal inhibitors of human steroid 5α-reductase 1. *J. Med. Chem.* **2004**, *47*, 3546–3560.

(25) Fröhner, W.; Monse, B.; Braxmeier, T. M.; Casiraghi, L.; Sahagún, H.; Seneci, P. Regiospecific synthesis of mono-*N*-substituted indolopyrrolocarbazoles. *Org. Lett.* **2005**, *7*, 4573–4576.

(26) Bach, T.; Grosch, B.; Strassner, T.; Herdtweck, E. Enantioselective [6π]-photocyclization reaction of an acrylanilide mediated by a chiral host. Interplay between enantioselective ring closure and enantioselective protonation. *J. Org. Chem.* **2003**, *68*, 1107–1116.

(27) Adams, N. D.; Darcy, M. G.; Dhanak, D.; Duffy, K. J.; Fitch, D. M.; Knight, S. D.; Newlander, K. A.; Shaw, A. N. Compounds, compositions and methods. PCT Int. Appl. WO2006113432, 2006.

(28) (a) Denner, K.; Bernhardt, R. Inhibition studies of steroid conversions mediated by human CYP11B1 and CYP11B2 expressed in cell cultures. In *Oxygen Homeostasis and Its Dynamics*, 1st ed.; Ishimura, Y., Shimada, H., Suematsu, M., Eds.; Springer-Verlag: Tokyo, Berlin, Heidelberg, New York, 1998; pp 231−236. (b) Denner, K.; Doehmer, J.; Bernhardt, R. Cloning of CYP11B1 and CYP11B2 from normal human adrenal and their functional expression in COS-7 and V79 chinese hamster cells. *Endocr. Res.* **1995**, *21*, 443–448. (c) Böttner, B.; Denner, K.; Bernhardt, R. Conferring aldosterone synthesis to human CYP11B1 by replacing key amino acid residues with CYP11B2-specific ones. *Eur. J. Biochem.* **1998**, *252*, 458–466.

(29) Lamberts, S. W.; Bruining, H. A.; Marzouk, H.; Zuiderwijk, J.; Uitterlinden, P.; Blijd, J. J.; Hackeng, W. H.; de Jong, F. H. The new aromatase inhibitor CGS-16949A suppresses aldosterone and cortisol production by human adrenal cells in vitro. *J. Clin. Endocrinol. Metab.* **1989**, *69*, 896–901.

(30) Demers, L. M.; Melby, J. C.; Wilson, T. E.; Lipton, A.; Harvey, H. A.; Santen, R. J. The effects of CGS 16949A, an aromatase inhibitor on adrenal mineralocorticoid biosynthesis. *J. Clin. Endocrinol. Metab* **1990**, *70*, 1162–1166.

(31) Heim, R.; Lucas, S.; Grombein, C. M.; Ries, C.; Schewe, K. E.; Negri, M.; Müller-Vieira, U.; Birk, B.; Hartmann, R. W. Overcoming undesirable CYP1A2 inhibition of pyridylnaphthalene type aldosterone synthase inhibitors: Influence of heteroaryl derivatization on potency and selectivity. *J. Med. Chem.* **2008**, *51*, 5064–5074.

(32) (a) Ehmer, P. B.; Jose, J.; Hartmann, R. W. Development of a simple and rapid assay for the evaluation of inhibitors of human 17α-hydroxylase-$C_{17,20}$-lyase (P450c17) by coexpression of P450c17 with NADPH-cytochrome-P450-reductase in *Escherichia coli*. *J. Steroid Biochem. Mol. Biol* **2000**, *75*, 57–63. (b) Hutschenreuter, T. U.; Ehmer, P. B.; Hartmann, R. W. Synthesis of hydroxy derivatives of highly potent nonsteroidal CYP17 inhibitors as potential metabolites and evaluation of their activity by a noncellular assay using recombinant enzyme. *J. Enzyme Inhib. Med. Chem.* **2004**, *19*, 17–32.

(33) Thompson, E. A.; Siiteri, P. K. Utilization of oxygen and reduced nicotinamide adenine dinucleotide phosphate by human placental microsomes during aromatization of androstenedione. *J. Biol. Chem.* **1974**, *249*, 5364–5372.

(34) Hartmann, R. W.; Batzl, C. Aromatase inhibitors. Synthesis and evaluation of mammary tumor inhibiting activity of 3-alkylated 3-(4-aminophenyl)piperidine-2,6-diones. *J. Med. Chem.* **1986**, *29*, 1362–1369.

(35) Taymans, S. E.; Pack, S.; Pak, E.; Torpy, D. J.; Zhuang, Z.; Stratakis, C. A. Human CYP11B2 (aldosterone synthase) maps to chromosome 8q24.3. *J. Clin. Endocrinol. Metab.* **1998**, *83*, 1033–1036.

(36) (a) Chohan, K. K.; Paine, S. W.; Mistry, J.; Barton, P.; Davis, A. M. A rapid computational filter for cytochrome P450 1A2 inhibition potential of compound libraries. *J. Med. Chem.* **2005**, *48*, 5154–5161. (b) Korhonen, L. E.; Rahnasto, M.; Mähönen, N. J.; Wittekindt, C.; Poso, A.; Juvonen, R. O.; Raunio, H. Predictive three-dimensional quantitative structure−activity relationship of cytochrome P450 1A2 inhibitors. *J. Med. Chem.* **2005**, *48*, 3808–3815.

(37) Butler, M. A.; Iwasaki, M.; Guengerich, F. P.; Kadlubar, F. F. Human cytochrome P-450$_{PA}$ (P-450IA2), the phenacetin *O*-deethylase, is primarily responsible for the hepatic 3-demethylation of caffeine and *N*-oxidation of carcinogenic arylamines. *Proc. Natl. Acad. Sci. U.S.A.* **1989**, *86*, 7696–7700.

(38) Sesardic, D.; Boobis, A. R.; Murray, B. P.; Murray, S.; Segura, J.; de la Torre, R.; Davies, D. S. Furafylline is a potent and selective inhibitor of cytochrome P450IA2 in man. *Br. J. Clin. Pharmacol.* **1990**, *29*, 651–663.

(39) Ulmschneider, S.; Negri, M.; Voets, M.; Hartmann, R. W. Development and evaluation of a pharmacophore model for inhibitors of aldosterone synthase (CYP11B2). *Bioorg. Med. Chem. Lett.* **2006**, *16*, 25–30.

(40) Ries, C.; Lucas, S.; Heim, R.; Birk, B.; Hartmann, R. W. Selective aldosterone synthase inhibitors reduce aldosterone formation in vitro and in vivo. *J. Steroid Biochem. Mol. Biol.* **2008**, submitted for publication.

(41) Häusler, A.; Monnet, G.; Borer, C.; Bhatnagar, A. S. Evidence that corticosterone is not an obligatory intermediate in aldosterone biosynthesis in the rat adrenal. *J. Steroid Biochem.* **1989**, *34*, 567–570.

JM800888Q